Applied Radiation and Isotopes 168 (2021) 109551

Contents lists available at ScienceDirect

Applied Radiation and Isotopes

journal homepage: http://www.elsevier.com/locate/apradiso

Polonium behavior following a vacuum window rupture in a lead-bismuth eutectic based accelerator driven system

Erik Karlsson [a,b], Jörg Neuhausen [a,*], Alexander Aerts [c], Ivan I. Danilov [a,b], Robert Eichler [a,b], Andreas Türler [b], Alexander Vögele [a]

[a] Paul Scherrer Institut, Forschungsstrasse 111, 5232, Villigen PSI, Switzerland
[b] University of Bern, Freiestrasse 3, 3012, Bern, Switzerland
[c] SCK·CEN, Boeretang 200, 2400, Mol, Belgium

ARTICLE INFO

Keywords:
Accelerator driven system
Polonium
Lead-bismuth eutectic
Stainless steel
Transmutation
Vacuum
Thermochromatography
Adsorption

ABSTRACT

Accelerator driven fast nuclear reactors cooled by lead-bismuth eutectic (LBE) are developed for transmuting long-lived radionuclides in spent nuclear fuel. Due to the nature of the coolant, operating the reactor will result in a production of ^{210}Po by neutron capture. Understanding the behavior of this highly radiotoxic nuclide in the event of a failure of the window separating the evacuated proton beam guide from the reactor core is required for safety assessments. The present work aims at acquiring this knowledge by studying the evaporation of polonium from neutron-irradiated LBE and its deposition in a scaled down model of the beam tube. Experimental results along with Monte Carlo simulations indicate that polonium adsorbs as a single species with an adsorption enthalpy of approximately −156 kJ/mol.

1. Introduction

There are currently about 450 operating civilian nuclear reactors world-wide producing electricity with comparably low CO_2 emissions. However, the problem with the existing nuclear fleet is the highly radioactive waste as well as the potential long term effects of technical failure. For the moment the solutions brought forward for the nuclear waste are based on long-term storage. The required storage times for high-level radioactive waste to decay to a negligible radiological hazard exceed 100 ka. During this time the integrity of the storage facility must be guaranteed to avoid release of radionuclides into the surrounding environment.

Several innovative reactor designs have been suggested to address these problems. These designs offer improved safety, increased utilization of the fuel and a much reduced amount of end-of-cycle waste in part due to transmutation (EURATOM, 2017). The present work is centered on a particular sub-group of these designs, the lead-bismuth eutectic (LBE, 55.5%/44.5% Bi/Pb) cooled accelerator driven fast reactor. What sets this type of reactor apart from currently existing ones is the ability to utilize the nuclear fuel to a higher burn-up than what is achieved using thermal neutrons as well as conventional fast reactors. Through breeding and with a fast neutron spectrum, fertile nuclides, such as e. g. ^{238}U, can be utilized and minor actinides fissioned. Additionally, loss of coolant from boiling is nearly impossible due to the very high boiling point. Another advantage is the possibility to remove decay heat via passive convection cooling.

The accelerator driven system (ADS) reactor concept is based on loading the reactor fuel in such a way that $k_{eff} \ll 1$, however the neutron economy is balanced by addition of neutrons from an external source (Rubbia, 1995). In the case studied here, the source is an accelerator which accelerates protons to a high energy (600 MeV). These protons are injected into an evacuated beam guide going from the top of the reactor vessel down into the core. Once inside the core they pass through a thin metallic window and impact the lead and bismuth in the coolant yielding neutrons from nuclear spallation reactions. The neutron yield for this system is helped by the high-Z coolant as well as secondary (n, xn) reactions that add to the neutron generation cascade (Heidet et al., 2015; Lone and Wong, 1995). If the fuel has a high burnup, the proton flux can be adjusted to account for this, keeping the reactor critical for a longer time without refueling. Further valuable safety features include the ability to completely scram the reactor in milliseconds by interrupting the proton beam and thus quickly stopping the chain reaction. The decay heat removal is possible by passive convection without the use of pumps. All these features greatly enhance the safety of the reactor

* Corresponding author. Laboratory of Radiochemistry, Paul Scherrer Institut, Forschungsstrasse 111, 5232, Villigen PSI, Switzerland.
E-mail address: joerg.neuhausen@psi.ch (J. Neuhausen).

https://doi.org/10.1016/j.apradiso.2020.109551
Received 31 March 2020; Received in revised form 24 September 2020; Accepted 30 November 2020
Available online 4 December 2020

compared to a normal water-cooled system and considerably reduce the production of long-lived highly radioactive waste.

In addition to the neutron producing spallation reaction in the core, other spallation, fission and activation reactions are simultaneously taking place producing a large variety of nuclides. Assessments made on the full nuclide inventory of the reactor as well as the potential radiological impact of an unmitigated release identifies the main safety-relevant nuclide as ^{210}Po (Saito et al., 2002). This nuclide is produced in a variety of different ways but the dominant reaction is the direct neutron capture of ^{209}Bi:

$^{209}\mathrm{Bi} + \mathrm{n} \rightarrow {}^{210}\mathrm{Bi}\ (\beta^-,\ 5.01\ \mathrm{days}) \rightarrow {}^{210}\mathrm{Po}$

There is also the possibility of a proton capture reaction which produces several different polonium isotopes, including ^{210}Po through the (p, xn) reaction with ^{209}Bi:

$^{209}\mathrm{Bi} + \mathrm{p} \rightarrow {}^{210-x}\mathrm{Po} + \mathrm{x\ n}\ (\mathrm{x} = 0\ \mathrm{to}\ 8).$

After activation by neutron capture, the initially produced bismuth isotope decays with a half-life of about five days into polonium. The ^{210}Po isotope which results from the decay has a half-life of about 138 days and decays into stable ^{206}Pb (Nucleonica GmbH, 2019). While the ^{209}Bi cross-section for neutron capture is not particularly large (<10 mb between the resonance region and the epithermal region), the neutron flux is very intense and the target is plentiful (Soppera et al., 2014). In comparison, the cross section for ^{210}Po formation via proton induced reactions is still smaller (<20 μb for proton energies between 8.95 and 21.95 MeV (Choudhury and Lahiri, 2018). For a normally operating reactor of this kind, an expected steady-state polonium inventory may be in the range of several kilograms (OECD and Nuclear Energy Agency, 2015). The expected presence of such a large amount of a highly radiotoxic nuclide requires investigation to determine the potential release in the event of an accident. Therefore, a considerable amount of work has been performed investigating the release of polonium from LBE, starting with studies supporting the development of LBE-cooled reactors used in nuclear submarines in the 1960s and continued in the last decades, triggered by the growing interest in LBE-cooled breeder and transmuter systems. A review of this work including a discussion of the mechanisms of polonium release from LBE can be found in reference (Aerts et al., 2019).

The mode of release concerned in this work is a break in the window separating the environment of the proton beam guide from the LBE coolant itself. Such a break would expose the LBE to the vacuum of the beam guide initiating an evaporation of the polonium species present potentially allowing migration into the accelerator. The intention of this work is to study the transport and deposition of polonium in a vacuum thermochromatography setup that resembles the conditions prevailing in the beam guide of an ADS.

2. Methods

2.1. Vacuum thermochromatography

The classical thermochromatographic method is based on determining the strength of interaction of gaseous chemical species transported in an inert or reactive laminar gas flow with a stationary surface material in a negative temperature gradient. This allows for separating the occurring chemical species based on their affinity to the chosen surface material. Thermochromatographic experiments on LBE containing ^{206}Po in various gas atmospheres have been performed by Gonzalez Prieto et al. (Gonzalez Prieto et al., 2015). The purpose of these experiments was to determine the evaporation behavior of polonium evaporated from the LBE into the cover gas as well as its subsequent deposition. These results point to the polonium speciation being dependent on the moisture content as well as the reduction/oxidation potential of the gas. In a dry oxygen atmosphere the polonium likely deposits as polonium dioxide at very high temperatures (550–650 °C). In a dry inert helium atmosphere the species is assumed to be PbPo and the determined adsorption enthalpy is −160 ± 10 kJ/mol (Gonzalez Prieto et al., 2015).

At the vacuum thermochromatographic conditions without any carrier gas applied in this work, the polonium is evaporated inside a column and then allowed to move at free molecular flow conditions stochastically inside the column through alternating adsorption and desorption reactions. Due to the adsorption time increasing when the column surface temperature decreases, this introduces retention and thus accumulation of polonium species in certain parts of the column. When the experiment is concluded by ceasing the heating of the column, this increased residence time at lower temperatures will have produced a deposition pattern. From this pattern, adsorption interaction data can be extracted using Monte Carlo simulation by altering one parameter (the interaction strength) in an iterative fashion until the simulation agrees with experimental data.

2.2. Monte Carlo simulation

The simulation of vacuum thermochromatography is based on the methodology developed by I. Zvara (2008). This microscopic kinetic model requires some assumptions to be made about the applied experimental system. The simulation assumes we have Knudsen diffusion occurring in the system, meaning that the mean free path of the particles is greater than the system dimensions. For a detailed description of how this is calculated see (Pfeiffer Vacuum, 2013). The Langmuir adsorption model is considered to be partially valid. Equivalent adsorption sites are assumed as well as there being neither interactions between molecules of the adsorbed species nor two dimensional surface movement of adsorbed species. Movement inside the column is simulated in discrete steps where the volatilized particle (atom or molecule) of the chemical species moves along a straight line from one point on the column surface to another. Upon intersection of this path with the surface, the species can either adsorb or bounce away again. The fraction of intersections resulting in an adsorption is known as the sticking factor (ϵ), which is a property that is specific to each species-surface pairing. Evaporation experiments performed using tellurium as an analogue of polonium determined a value of approximately $\epsilon = 0.24$ (Michelato et al., 2007). This value was applied in the Monte Carlo simulation used for the determination of the adsorption enthalpy. When desorption of a particle occurs, the trajectory of the particle in the longitudinal direction of the column is determined by an angle in relation to the surface normal. This angle is selected randomly from a distribution based on the Knudsen cosine law. The consequence of this is as follows: The probability of a particle desorbing from an ideal flat surface at an angle θ with the surface normal is proportional to sin 2θ (Knudsen, 1909). This suppresses the largest and smallest angles and makes 45° ($\pi/4$) angle with the surface normal the most probable angle of desorption. Additionally, the same holds for a surface with an uneven micro-geometry such as for example stainless steel (Feres and Yablonsky, 2014). For a particle which impacted the surface but did not stick, a new scattering angle from the same angular distribution is calculated without assuming an elastic collision with the surface.

In the present experiments the LBE vapor pressure at the sample temperature remains around 10^{-5} mbar (OECD and Nuclear Energy Agency, 2015). This pressure corresponds to a mean free path exceeding our column dimensions meaning Knudsen diffusion can be assumed for the whole system (Pfeiffer Vacuum, 2013).

3. Experimental

To construct the scale model of an ADS beam guide (see Fig. 1), a column of stainless steel 316L (SS316L, Sandvik/Swagelok Lot: 35828) was selected. The 316L is a low carbon austenitic stainless steel with good corrosion resistance against LBE. This particular steel is a material commonly suggested for use in lead and lead-bismuth fast reactors (Séran and Le Flem, 2017). The dimensions of the column were an inside diameter of 4 mm, a length of 1100 mm and a wall thickness of 1 mm. To

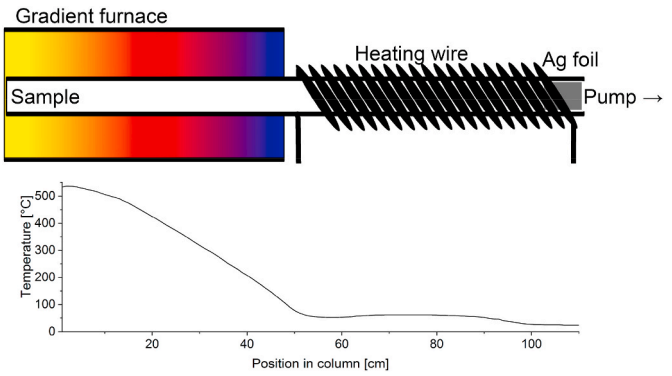

Fig. 1. (top) Sketch of gradient furnace and heating wire setup showing a general overview of the experiment. To the right the vacuum pump is connected. Just before the pump a silver foil is placed to capture volatile species. The sample is located to the left at the sealed hot end of the column. (bottom) At the peak the gradient reaches a temperature of 540 °C, falling to ~50 °C which is kept through the isothermal section produced by the heating wire. The silver foil is located at the exit of the column where the temperature is at the ambient level.

replicate the temperature conditions present in a beam guide, a gradient furnace was utilized to give a smooth tapering gradient down from the temperature in the evaporation zone (~540 °C) to a heated isothermal section. The isothermal section had a temperature of approximately 50 °C, which was achieved using heating wire wrapped around the outside of the column. The column was closed by welding a 4 mm diameter SS316L plug at one end. At the other end a ~1 cm wide strip of metallic silver foil was inserted to adsorb trace polonium potentially escaping the system. To continuously evacuate the system to pressures below 10^{-5} mbar, a turbomolecular vacuum pump (Hicube®, Pfeiffer) was attached at the open end of the column.

To avoid disturbing the gradient while it is measured by small convective heat transfer that would not be present in the experiment, a way was devised to measure the gradient with the column evacuated. The pump was attached at one end of the column and at the other end a thermocouple (K-type) was introduced through a septum in the form of an O-ring seal inserted into a Swagelok® connector. This enabled a high enough vacuum to be present (10^{-4} mbar) while measuring the gradient stepwise through insertion and retraction of the thermocouple.

To produce starting samples for the experiments, lead-bismuth eutectic 55.5/44.5% Bi/Pb supplied by SIDECH (purity 99.999%) was wrapped in a tantalum foil and placed in a fused silica tube that was evacuated and subsequently heated to 1000 °C overnight to reduce the oxygen content of the LBE. Small pieces of the reduced LBE were irradiated at the Paul Scherrer Institute SINQ-NIS pneumatic rabbit irradiation facility by thermalized spallation neutrons to produce polonium directly in the LBE matrix. In total, 250 mg of LBE was irradiated for 10,680 s at a thermal neutron flux of approximately 10^{13} n/(s cm^2). The mass and irradiation time was chosen for the activity not to exceed regulatory limits.

The 250 mg piece of LBE was cut into smaller samplings weighing 65 mg, 75 mg, and 85 mg, respectively. Before each experiment the sample was inserted into the open end of the steel column held vertically and allowed to fall down to rest on the plug at the closed end. To verify the position of the sample a hand-held radiation monitor was used to detect the γ-emitting nuclides also produced by the irradiation (mainly bismuth isotopes).

The column was then inserted horizontally into the thermochromatography setup. After connecting the column to the vacuum pump, a vacuum of approximately 10^{-6} mbar was achieved before heating was commenced. To ensure sufficient evaporation of polonium from the LBE as well as minimize the influence of the time it takes for the temperature gradient to establish, an experimental time of 72 h was selected. This was chosen as a low fractional evaporation per hour was expected, however vacuum conditions increased the driving force (Gonzalez Prieto et al., 2014a). The gradient furnace was controlled with a temperature controller while the heating wire was operated via a manually pre-set voltage on a variable autotransformer.

Upon expiration of the experimental time the heating was turned off, followed by the vacuum pump once the system had cooled down. To analyze the polonium deposition in the column it was cut into 1 cm long pieces which were leached in 7M HNO_3 to dissolve the polonium. The leaching solutions were later mixed with scintillation cocktail (Ultima Gold™, PerkinElmer) in a scintillation vial. Each vial was measured by liquid scintillation counting (LSC) using a Packard Tri-Carb 3110TR, either for 2 h or until the 2σ uncertainty fell below 1%. The silver foils were rolled out flat and measured in an α-spectrometer (Canberra A450-18AM, data acquisition system Genie2k®). Absolute quantification from the latter measurement was found to be difficult because the deposition on the silver foils was not uniform and thus the measurement geometry turned out to be not reproducible. Due to this issue the foils were dissolved in 3.5 M HNO_3 and were also measured using LSC to determine the polonium content.

The quantitative LSC measurements of these foils experienced a quite severe color quench due to the large amount of dissolved silver. This was corrected for by using a ^{210}Pb standard solution with a known amount of silver added.

4. Results and discussion

The resulting irradiated LBE contained ^{210}Po with a mole fraction around $5{\cdot}10^{-10}$ (~80 Bq/mg). This value is much lower than the estimated steady-state mole fraction in the coolant of approximately 10^{-7} (Fiorito et al., 2018). However, for both concentrations ideal dilute behavior may be assumed.

From a qualitative as well as a quantitative point of view the conducted experiments produced very similar results. The resulting deposition pattern constructed from the LSC data are presented in Fig. 2. The bulk of the polonium forms a peak at roughly 200 °C with a pronounced tailing toward the hot end of the chromatography column. The deposition pattern indicates the presence of a single species being evaporated and deposited.

Through Monte Carlo simulation the adsorption enthalpy of the species deposited around 200 °C on SS316L was determined to be −156 ± 5 kJ/mol.

Additional Monte Carlo simulations conducted indicate that the sticking factor has little impact on the behavior of a species, unless it takes on a very small value (<0.05) at which point the deposition shape changes. The change occurs through a broadening on mainly the colder side of the peak, whereas a feature of the measured deposition is a sharp edge toward the cold side. In Fig. 3 this is illustrated more clearly. Here

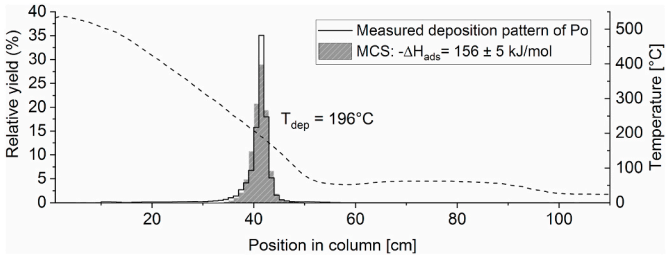

Fig. 2. Deposition pattern of ^{210}Po from vacuum thermochromatography experiments (black solid line) showing the main deposition at ~200 °C resulting in an adsorption enthalpy of −156 ± 5 kJ/mol determined using Monte Carlo simulation (hatched). The temperature gradient (dashed line) goes from 540 °C at the top and down in temperature before levelling out at around 50 °C for a nearly isothermal section between 20 and 60 cm from the pump before reaching room temperature.

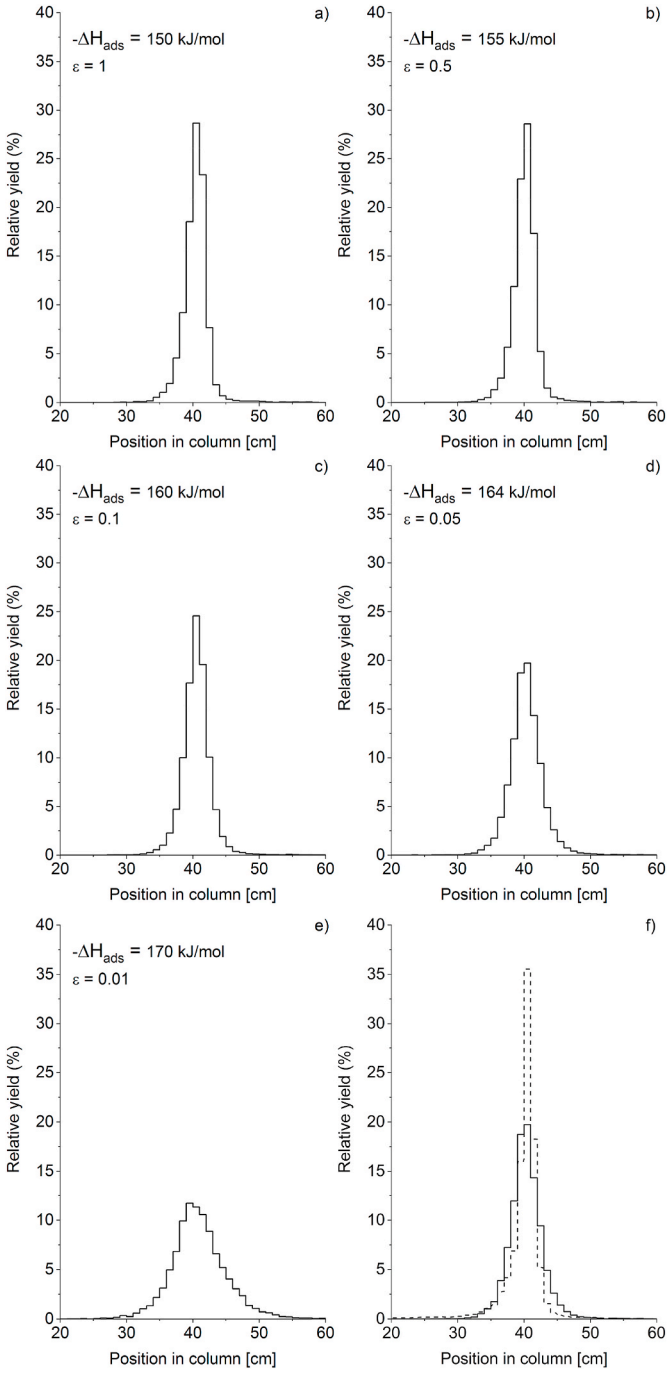

Fig. 3. Simulation results for different sticking factors ε with the Hads adjusted to produce a peak centered on the experimental peak. In a-e) the effect of a decreasing sticking factor is showcased with the peak becoming increasingly broadened. In f) a simulation result with sticking factor 0.05 (black line) is compared against the experimental result (dashed line) showing divergence from the experimentally observed behavior.

the simulation results for varying sticking factors and adsorption enthalpies are presented. The main goal of the simulations here was to produce a peak with its maximum in line with the experimental results for a given sticking factor by adjusting the adsorption enthalpy. This was done to clearly showcase that the shape of the peak is the main indicator of sticking behavior. The combinations of very low sticking factors and higher adsorption enthalpies produce peaks that significantly differ in shape from the experimental results. From the results presented in Fig. 3, it was possible to conclude the absence of a stronger adsorbing species ($-\Delta H_{ads} > 165$ kJ/mol) with a sticking factor less than 0.05.

The value determined for the adsorption enthalpy in the present experiments is very similar to that obtained in thermochromatography experiments in SS316L columns in helium carrier gas (Gonzalez Prieto et al., 2015), indicating that the deposited polonium species in both experiments is the same. In a recent quantum chemical study on the stability of gaseous polonium molecules (Mertens et al., 2019) it was found that among the polonium-containing gas phase species likely occurring over an LBE melt (PbPo, BiPo, Po and Po_2), lead polonide PbPo is the dominating species. This makes it plausible that this species is also the main species transported and deposited in the present experiment. Species containing two atoms of polonium such as the dimer Po_2 can be ruled out to occur in significant fractions both at the concentrations prevailing in an ADS and those of the present experiment. However, a safe speciation of the gaseous polonium species carrying only a single polonium atom actually occurring in the present experiments is not possible based on the adsorption properties alone.

The deposition pattern in Fig. 2 features a small tailing towards the colder side continuing for almost 40 cm. This likely continues throughout the whole column, but due to the detection limit of the LSC measurement the small amounts of ^{210}Po could not be detected on all sections from the low temperature part of the column. The detection limit was measured as approximately 2–3 cpm (counts per minute) exceeding the background level of 10–12 cpm. Polonium was however still present in the semi- quantitative α-spectrometry measurements of the silver foils.

From the LSC measurement of the silver foils it was determined that the polonium amount on the silver foil in all three experiments did not exceed 0.02% (~1 Bq) of the total amount in the system.

On the parts of the column in contact with the silver foil, a slightly elevated amount of polonium was measured as well. This is most likely due to mechanical abrasion of polonium adsorbed to the silver rather than spontaneous desorption from the silver during the experimental time, which is not possible due to the strong adsorption of Po on silver ($-\Delta H_{ads} = 216 \pm 7$ kJ/mol) (Maugeri et al., 2016).

In previous studies on the evaporation of polonium from LBE in an inert atmosphere the formation of a polonium species more volatile than elemental Po or lead and bismuth polonides has been observed that enhances polonium evaporation at temperatures lower than 500–600 °C (Rizzi et al., 2014). This species was later shown to originate from a surface oxide layer present on the polonium-containing LBE (Gonzalez Prieto et al., 2014b, 2016). While the samples in the current experiments have been reduced to remove dissolved oxygen, there is still a chance of oxygen contamination leading to formation of this volatile species. Therefore, it is important to determine whether the polonium depositing in the low-temperature region in the present experiments could originate from deposition of this more volatile species. For this purpose, we compare the experimentally determined deposition pattern and the results of the Monte Carlo simulation in more detail in a graph that shows the low temperature region at a magnified scale (Fig. 4). This comparison shows that the Monte Carlo simulation using the parameters of the experiment as well as the adsorption enthalpy extracted from it reproduces the behavior observed in the experiment very well without introducing any additional polonium species.

The low temperature deposition behavior observed is thus simply due to the large number of participating particles in the experiment. For any single particle the chance of a desorption or non-sticking impact event achieving a trajectory bound for the low temperature range is very small, but due to the large number of particles and events this process may lead to a deposition that can still be measured.

Thus, based on the absence of a secondary peak in the deposition pattern, as well as the presence of polonium in the low temperature part of the column and on the silver being fully explainable without an additional species, the experiments performed in this work confirm that either the volatile species observed in (Gonzalez Prieto et al., 2014b, 2016) adsorbs fairly strongly under the present conditions or the species

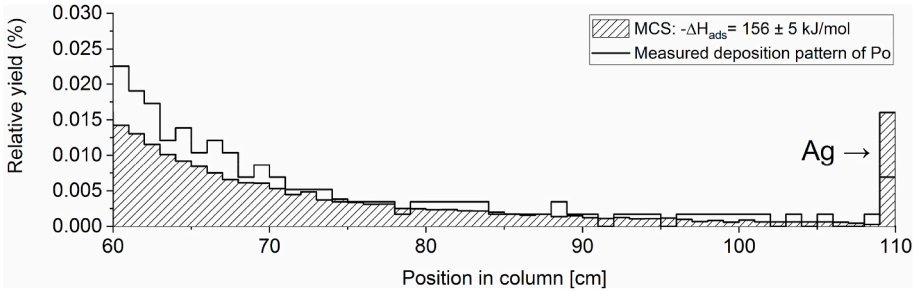

Fig. 4. Deposition pattern in the low temperature region (black line) from LSC measurement of experiment compared to the Monte Carlo simulation output (hatched) using the parameters of the experiment as well as the determined adsorption enthalpy. The step at the last centimeter in the simulation results is explained by a bunching up of the remaining tailing stretching beyond the end of the column.

is not formed in large enough amounts to be detected.

Additional simulations were performed to assess the time dependence of the release from the system. The observed Po adsorption behavior on steel was put into the simulation as a constant parameter and the experimental duration was varied. This was done to assess the time dependence of the release as well as the importance of fast interlocking systems to seal the beam guide quickly after a leak is detected. In these simulations the Po is assumed to be released from the LBE in an instantaneous pulse, meaning a variation in experiment time only influences the transport and not the evaporation. These simulations indicate that even after a very short time period there is some Po escaping from the column. Shortening the simulated break scenario from 72 h down to 1 min results in a reduction of the escaped Po out of the system by approximately 60%. This result may seem surprising, however most of the movement experienced by a particle throughout the transient occurs very early, whereas the majority of the scenario time it spends adsorbed at or near the final deposition point.

From looking at particle histories in the simulations, the most common location for a particle to start a completed system escaping jump is in the area of short adsorption times (high temperature), where the jumping is more frequent. Further down the column the geometry makes system escapes more likely due to the decreased distance to the opening, however the more important parameter for transmission/escape is the number of desorption events experienced per particle. In the low temperature zone where the geometry is more favorable a particle may only experience about ten jumps before the experiment duration expires. In contrast to this, in the high temperature area a single particle experiences thousands of such events each lasting a fraction of a millisecond. Each of these events carries a chance of the particle leaving the wall at a flat enough angle to escape the system.

Due to the low volatility of the evaporated component, our main focus to prevent Po escaping the system needs to be on the adjustment of the systems geometrical dimensions. These need to be carefully chosen not to permit the release of Po without any adsorption retention (i.e. without some surface encounters) beyond a certain fraction. For as long as there exists a free path between the deposition point and the system exit there will be escape events depending on the L/d ratio of the beam line. In the Monte Carlo simulation model the jump length in the y-direction (along the column) for each deposited particle is directly proportional to the column diameter as such:

$$l_y = d\,\frac{\cos\theta\,\sin\theta\,\sin\phi}{1-\sin^2\theta\,\sin^2\phi} \tag{1}$$

Here l_y is the jump length in the y-direction, angle θ is given by a random selection from the Knudsen cosine distribution between 0 and π/2, and ϕ is a random angle between 0 and 2π. Larger and smaller desorption angles θ are suppressed by the distribution but not fully eliminated. Depicted in Fig. 5 is the behavior for the studied system but with differing column diameters to show the reduction in escaped particles along with the increase of the length over diameter ratio.

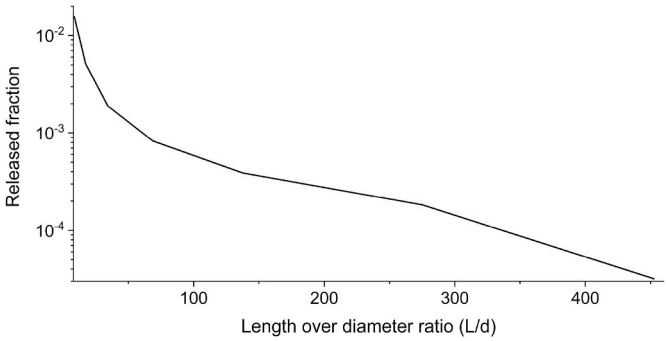

Fig. 5. Monte Carlo simulation outputs (black line) regarding the fully released fraction in columns of varying diameters for a 72 h experimental time. The length is kept fixed so as to not alter the temperature gradient. The graph depicts a variation from L/d of about 8.6–450.

Additional information can be extracted from assessing the β-activity deposited in the columns of the three experiments. A plot of the β-activity distribution in the columns is shown in Fig. 6. Toward the hot end we have two peaks that can be attributed to β-emitting nuclides. Since at the time of measurements all potentially measurable lead isotopes had already decayed, these can be assigned to bismuth isotopes present in the system, for example ^{205,206}Bi ($t_{1/2}$ = 14.9 and 6.2 d, respectively) as well as some remaining ^{210}Bi in the first two experiments. We can state that the bismuth peaks are very well separated from the main polonium deposition. We also have to consider that a low temperature tailing similar to that observed for polonium will probably also occur for lead and bismuth according to the Clausius-Clapeyron equation. However, due to the fast release and much higher volatility of lead polonide compared to lead and bismuth, we expect that the polonium release

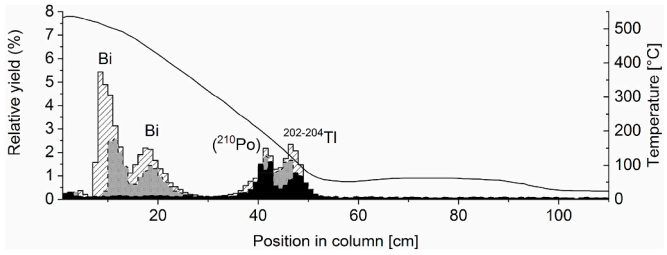

Fig. 6. β-activity deposition patterns from the three experiments. Results of experiments No. 1, 2 and 3 are shown as hatched, grey and black patterns, respectively. The experiments were performed in quick succession, however measurements for experiments one and two were conducted one week apart with the third following eight months later. From these times it can be concluded that the leftmost two peaks are of shorter half-life nuclides ($^{205\text{-}206,210}$Bi) whereas the two on the right come from longer lived sources. (^{202,204}Tl, possible misidentified ^{210}Po α-decay).

from LBE and deposition at 200 °C has already taken place before substantial amounts of lead and/or bismuth could have been accumulated at this position. From observing the LSC results of the β-depositions in the experiments, a much larger deposition (excluded from Fig. 6 to enhance visibility) was also observed at the sample point. This is assumed to be residual unevaporated LBE, indicating that only a fractional evaporation of the LBE occurs even after 72 h. Unfortunately, due to the continuous decay of bismuth during the measurement as well as potential activity contribution from other nuclides the evaporated amount could not be reliably quantified. These results support our assumption that the polonium is interacting with the steel surface and not LBE or bismuth deposited on steel.

The reason why two bismuth depositions are found at high temperature is not fully understood yet. If the deposition process was based on adsorption, the two depositions could be attributed to two different molecular species such as mono- and diatomic bismuth, adsorbing at specific temperatures/positions. However, with the relatively large amounts of bismuth present in the system one would rather expect depositions larger than a monolayer that would correspond to a deposition based on condensation rather than adsorption. This effect remains to be explained through further studies.

An additional feature of the β-activity deposition pattern is a peak at roughly 100 °C attributed to ^{202}Tl and ^{204}Tl. This attribution is based on the apparent long half-life (due to ^{204}Tl, $T_{1/2} = 3.78$ a) as it was still present in the third experiment, as well as the volatility. In previous irradiations of LBE, thallium has been observed as a nuclear reaction product. Previous experiments on the adsorption of thallium indicates a strong affinity for the elemental species to an oxide surface, which is why we tentatively rather assign this peak to TlOH (Serov et al., 2013). Next to the thallium peak there is a peak attributed to the instrument misidentifying a small fraction of α-decay events from ^{210}Po as beta decay.

5. Conclusions

From the results of this scaled down investigation of a design base accident compromising the integrity of an ADS beam guide one can conclude the following: Polonium evaporates from the exposed LBE surface as a single species that is not particularly volatile (likely PbPo). This is confirmed by Monte-Carlo simulations which reproduce the outcome of the experiments assuming only one species. This species was found to adsorb to an SS316L surface with an adsorption enthalpy of -156 ± 5 kJ/mol. The species cannot contain more than one polonium atom as the mole fraction is too low. Gibbs energy minimization calculations of the system in question indicate that orders of magnitude more polonium has to be present before dimers appear in a significant quantity. Therefore, the polonium in the produced LBE sample can be expected to behave similarly to the reactor case. In conclusion, the physicochemical data acquired here are directly applicable in safety studies assessing the polonium behavior in LBE-cooled nuclear reactors.

Author statement

Erik Karlsson: Conceptualization, Methodology, Software, Validation, Formal analysis, Investigation, Writing - Original Draft, Visualization; Jörg Neuhausen: Conceptualization, Validation, Data Curation, Writing - Review & Editing, Visualization, Supervision, Project administration, Funding acquisition; Alexander Aerts: Conceptualization, Formal analysis, Writing - Review & Editing; Robert Eichler: Validation, Methodology, Software, Writing - Review & Editing, Visualization; Ivan Danilov: Methodology, Resources; Alexander Vögele: Methodology, Resources; Andreas Türler: Validation, Writing - Review & Editing, Supervision

Funding

This work was supported by the European Commission within the project MYRTE under EURATOM HORIZON2020 Grant No. 662186.

Data availability

The raw data required to reproduce these findings cannot be shared at this time due to legal or ethical reasons. The processed data required to reproduce these findings cannot be shared at this time due to legal or ethical reasons.

Declaration of competing interest

The authors declare that they have no known competing financial interests or personal relationships that could have appeared to influence the work reported in this paper.

References

Aerts, A., Gonzalez Prieto, B., Neuhausen, J., 2019. Behaviour of Spallation, Activation and Fission Products in LBE, Reference Module in Materials Science and Materials Engineering. Elsevier. https://doi.org/10.1016/B978-0-12-803581-8.11612-1.

Nucleonica GmbH, 2019. Nuclide Datasheets. Nucleonica Nuclear Science Portal. Nucleonica GmbH, Karlsruhe, Germany, 3.0.151.0001. www.nucleonica.com.

Choudhury, D., Lahiri, S., 2018. Estimation of polonium radionuclides in proton irradiated lead-bismuth eutectic (LBE) targets by LSC-TDCR technique and gamma spectrometry. Eur. Phys. J. A 54, 212–219. https://doi.org/10.1140/epja/i2018-12646-7.

EURATOM, 2017. Euratom Contribution to the Generation IV International Forum Systems in the Period 2005-2014 and Future Outlook, EUR 28391 EN. Publications Office of the European Union, Luxembourg. http://doi.org/10.2760/256957.

Feres, R., Yablonsky, G., 2014. Knudsen's cosine law and random billiards. Chem. Eng. Sci. 59, 1541–1556. https://doi.org/10.1016/j.ces.2004.01.016.

Fiorito, L., Stankovskiy, A., Hernandez-Solis, A., Van den Eynde, G., Žerovnik, G., 2018. Nuclear data uncertainty analysis for the Po-210 production in MYRRHA. EPJ Nuclear Sci. Technol. 4, 48. https://doi.org/10.1051/epjn/2018044.

Gonzalez Prieto, B., Marino, A., Lim, J., Rosseel, K., Martens, J., Rizzi, M., Neuhausen, J., Van den Bosch, J., Aerts, A., 2014a. Use of the transpiration method to study polonium evaporation from liquid lead-bismuth eutectic at high temperature. Radiochim. Acta 102 (12), 1083–1091. https://doi.org/10.1515/ract-2014-2263.

Gonzalez Prieto, B., Lim, J., Mariën, A., Rosseel, K., Martens, J.A., Van den Bosch, J., Neuhausen, J., Aerts, A., 2014b. Non-uniform polonium distribution in lead–bismuth eutectic revealed by evaporation experiments. J. Radioanal. Nucl. Chem. 302 (1), 195–200. https://doi.org/10.1007/s10967-014-3264-1.

Gonzalez Prieto, B., Neuhausen, J., Eichler, R., Vögele, A., Piguet, D., Schumann, D., 2015. Interaction of Polonium Released from Lead-Bismuth Eutectic with Stainless Steel and Fused Silica in Dry Gaseous Atmospheres. LCH Annual Report 2015, Villigen PSI, Switzerland.

Gonzalez Prieto, B., Lim, J., Rosseel, K., Martens, J.A., Aerts, A., 2016. Polonium evaporation from liquid lead–bismuth eutectic with different oxygen content. J. Radioanal. Nucl. Chem. 309 (2), 597–605. https://doi.org/10.1007/s10967-015-4670-8.

Heidet, F., Brown, N.R., H Tajar, M., 2015. Accelerator-reactor coupling for energy production in advanced nuclear fuel cycles. Rev. Accel. Sci. Technol. 8, 99–114. https://doi.org/10.1142/S1793626815300066.

Knudsen, M., 1909. Die Gesetze der Molekularströmung und der inneren Reibungsströmung der Gase durch Röhren. Ann. Phys. 333 (1), 75–130. https://doi.org/10.1002/andp.19093330106.

Lone, M.A., Wong, P.Y., 1995. Neutron yields from proton-induced spallation reactions in thick targets of lead. Nucl. Instrum. Methods A. 362, 499–505. https://doi.org/10.1016/0168-9002(95)00286-3.

Maugeri, E.A., Neuhausen, J., Misiak, R., Eichler, R., Dressler, R., Piguet, D., Vögele, A., Schumann, D., 2016. Adsorption of volatile polonium species on metals in various gas atmospheres: Part II – adsorption of volatile polonium on platinum, silver and palladium. Radiochim. Acta 104 (11), 769–779. https://doi.org/10.1515/ract-2016-2575.

Mertens, M.A.J., Aerts, A., Infante, I., Neuhausen, J., Cottenier, S., 2019. Po-containing molecules in fusion and fission reactors. J. Phys. Chem. Lett. 10 (11), 2879–2884. https://doi.org/10.1021/acs.jpclett.9b00824.

Michelato, P., Cavaliere, E., Pagani, C., Bari, E., Bonucci, A., 2007. Vacuum interface analysis of a windowless spallation target for accelerator-driven systems. Nucl. Sci. Eng. 157, 95–109. https://doi.org/10.13182/NSE07-A2715.

OECD and Nuclear Energy Agency, 2015. Handbook on lead-bismuth eutectic alloy and lead properties, materials compatibility, thermal-hydraulics and technologies. Organisation for Economic Co-Operation and Development. NEA No. 7268. https://doi.org/10.1787/42dcd531-en.

Pfeiffer Vacuum, 2013. The Vacuum Technology Book Volume II – Know How Book. Pfeiffer Vacuum GmbH, Asslar, Germany.

Rizzi, M., Neuhausen, J., Eichler, R., Türler, A., Mendonça, T.M., Stora, T., Gonzalez Prieto, B., Aerts, A., Schumann, D., 2014. Polonium evaporation from dilute liquid metal solutions. J. Nucl. Mater. 450, 304–313. https://doi.org/10.1016/j.jnucmat.2014.01.047.

Rubbia, C., 1995. A high gain energy amplifier operated with fast neutrons. AIP Conf. Proc. 346, 44–53. https://doi.org/10.1063/1.49069.

Saito, M., Stankovskii, A., Artisyuk, V., Korovin, Yu, Shmelev, A., Titarenko, Yu, 2002. Radiological hazard of spallation products in accelerator-driven system. Nucl. Sci. Eng. 142, 22–36. https://doi.org/10.13182/NSE02-A2284.

Séran, J.-L., Le Flem, M., 2017. Structural materials for generation IV nuclear reactors: 8 - irradiation-resistant austenitic steels as core materials for generation IV nuclear reactors. DEN, CEA Saclay, Université Paris Saclay, Gif sur Yvette, France, pp. 285–328. https://doi.org/10.1016/B978-0-08-100906-2.00008-2.

Serov, A., Eichler, R., Dressler, R., Piguet, D., Türler, A., Vögele, A., Wittwer, D., Gäggeler, H.W., 2013. Adsorption interaction of carrier-free thallium species with gold and quartz surfaces. Radiochim. Acta 101 (7), 421–425. https://doi.org/10.1524/ract.2013.2045.

Soppera, N., Bossant, M., Dupont, E., 2014. Janis 4: an improved version of the NEA java-based nuclear data information system. Nucl. Data Sheets 120, 294–296. https://doi.org/10.1016/j.nds.2014.07.071.

Zvara, I., 2008. The Inorganic Chemistry of Heavy Elements, first ed. https://doi.org/10.1007/978-1-4020-6602-3